

Onset of wavenumber bandgaps via alternating Willis coupling signs

Hasan B. Al Ba'ba'a

Department of Mechanical Engineering, Union College, Schenectady, NY 12308, USA
albabaah@union.edu

arXiv:2412.06798v1 [physics.optics] 22 Nov 2024

Abstract — This article introduces a methodology for inducing wavenumber bandgaps via alternating signs of Willis coupling. A non-reciprocal wave equation of Willis-type is considered, and the wave dispersion analyses are carried out via the transfer matrix method. Further, reversing Willis-coupling signs is proven to yield reciprocal band structures with wavenumber bandgaps, and their width and limits are analytically quantified. Similarities between materials with reversed-sign Willis coupling and bi-layered phononic crystals are noted, followed by concluding remarks.

Keywords — Wavenumber bandgaps, Willis coupling, non-reciprocal waves, periodic structures, dispersion diagram.

Background and motivation

Consider a non-reciprocal wave equation, in the absence of external forces [1]:

$$\frac{\partial^2 u}{\partial t^2} + 2v_0 \frac{\partial^2 u}{\partial x \partial t} + (v_0^2 - c^2) \frac{\partial^2 u}{\partial x^2} = 0, \quad (1)$$

governing longitudinal displacement $u(x, t)$ of an axially moving elastic rod, quantified along the direction x at any instant of time t . The wave speed in the elastic medium $c = \sqrt{E/\rho}$ is a function of its density ρ and modulus of elasticity E , and it is assumed to have a constant cross-sectional area A . Besides being of gyroscopic nature [2], Equation (1) is also known as a Willis-type equation of motion, where v_0 symbolizes the Willis coupling coefficient [3, 4], equivalent to the rod's speed [1]. Its non-reciprocity stems from the introduced momentum bias, evident from the mixed derivative term.

To examine wave dispersion and understand periodic structures governed by Equation (1), a transfer matrix that relates the state vectors (displacement and internal force) at the terminals of a segment of length ℓ is developed. By introducing $\nu = v_0/c$, $\tau = \omega_0 t$, and $\xi = x/\ell$ as the normalized modulation speed ($\nu \in [0, 1)$), non-dimensional time (with $\omega_0 = c(1 - \nu^2)/\ell$), and non-dimensional length, respectively, Equation (1) becomes:

$$(1 - \nu^2) \frac{\partial^2 u}{\partial \tau^2} + 2\nu \frac{\partial^2 u}{\partial \xi \partial \tau} - \frac{\partial^2 u}{\partial \xi^2} = 0 \quad (2)$$

Following the methodology in Ref. [1], the following unit-cell's transfer matrix is developed,

$$\mathbf{T}(\nu) = e^{i\nu\Omega\xi} \mathbf{Y}(\nu) \quad (3)$$

where the matrix $\mathbf{Y}(\nu)$, having a determinant of one, is given by:

$$\mathbf{Y}(\nu) = \begin{bmatrix} \cos(\Omega\xi) - i\nu \sin(\Omega\xi) & \frac{1}{k\Omega} \sin(\Omega\xi) \\ -(1 - \nu^2)k\Omega \sin(\Omega\xi) & \cos(\Omega\xi) + i\nu \sin(\Omega\xi) \end{bmatrix} \quad (4)$$

In Equations (3) and (4), $\Omega = \omega/\omega_0$ is a normalized version of excitation frequency ω , $k = EA/\ell$ is the equivalent longitudinal stiffness of the rod segment, and $i = \sqrt{-1}$ is the imaginary unit. The transfer matrix $\mathbf{T}(\nu)$ relates the state vectors at the terminals of a single unit cell at $\xi = 0$ ($x = 0$) and any length ξ according to $\mathbf{z}(\xi) = \mathbf{T}(\nu)\mathbf{z}(0)$, where the state vector $\mathbf{z}(\xi) = \{\bar{u}(\xi) f(\xi)\}^T$ compiles the displacement amplitude and internal force $f = ku_\xi$ at a given terminal of the unit cell.

Despite the introduction of a momentum bias, I next show the linearity of the dispersion relation from analyzing the eigenvalue of transfer matrix $\mathbf{T}(\nu)$ in Equation (3) with $\xi = 1$. Computing the determinant of $\mathbf{T}(\nu) - \lambda\mathbf{I}$, where λ is an eigenvalue and \mathbf{I} is a 2×2 identity matrix, and solving for λ produce the following solutions:

$$\lambda = e^{i\nu\Omega} \left(\frac{\text{tr}(\mathbf{Y})}{2} \pm i\sqrt{1 - \left(\frac{\text{tr}(\mathbf{Y})}{2}\right)^2} \right) \quad (5)$$

Consider now that the eigenvalues are written as $\lambda = e^{iq}$, where q is a non-dimensional wavenumber. The driven-wave dispersion relation is developed from Equation (5) after taking the natural logarithmic of both sides and executing a few mathematical manipulations:

$$q = q_s \pm \Omega \quad (6)$$

where $q_s = \nu\Omega$ is a wavenumber *phase shift*, reminiscent of the phase shift observed in Willis monatomic lattices recently developed by the author [5]. As evident from Equation (6), and in agreement with the results obtained in Ref. [1], the dispersion relation remains linear with Willis coupling (or rod's motion), yet its slope is unequal about the zero wavenumber and it changes as a function of the normalized modulation speed ν .

An additional observation I note here is that the angle at which the linear dispersion skews relative to the vertical axis can be analytically quantified via a straightforward trigonometry. More specifically, a triangle is formulated via the phase shift q_s and its corresponding frequency Ω as shown in Figure 1, from which the skew angle ϕ can be derived:

$$\phi = \tan^{-1}(\nu) \quad (7)$$

This skew angle ϕ grows non-linearly starting from $\nu = 0$, the reciprocal case, for which the triangle understandably collapses to a vertical line, and, unlike the phase shift q_s , is independent of the frequency Ω . A comparison between the reciprocal ($\nu = 0$) and a non-reciprocal ($\nu = 1/3$) cases are shown in Figure 1.

As detailed earlier, a homogeneous elastic rod with a single Willis coupling results in non-reciprocity. One might then wonder: What is the effect of having a periodic variation in Willis coupling? Unlike periodic variations in mechanical properties or placement of local resonators, which induce Bragg and/or locally resonant frequency bandgaps [6-8], a homogeneous elastic rod

with periodic variation in Willis coupling shall open wavenumber bandgaps, constituting the key finding in this study. The presented approach adds to the typical methods for initiating wavenumber bandgaps, encompassing structural damping [9], temporal stiffness modulation [10], supersonic spatiotemporal modulation [1], and the use of generally complex spatiotemporally harmonic functions for stiffness [11].

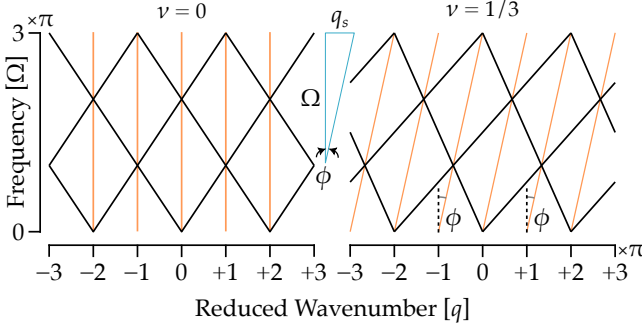


Figure 1: A comparison between reciprocal ($\nu = 0$) and non-reciprocal ($\nu = 1/3$) band structures, corresponding to the wave equation in Equation (1). The definition of the skew angle ϕ is illustrated via a triangle, constructed via the wavenumber phase shift q_s and its corresponding frequency Ω . Note that the dispersion relation is repeated periodically along the wavenumber axis for better visualization of the skew angle.

Elastic rod with periodic Willis coupling

Consider a unit cell of an elastic rod divided evenly into two segments as seen in Figure 2. Each segment has equivalent normalized length $\zeta = 1/2$, cross-sectional area, and material properties, yet a different Willis coupling. Reversed signs of Willis coupling are enforced to eliminate the skew angle ϕ of the resulting dispersion. Selecting this design is intended for drawing analogies with frequency bandgaps in a special class of phononic crystals as will be detailed shortly. Multiplying the transfer matrix of each segment using Equation (3), and denoting their Willis couplings as ν_- and ν_+ , results in the unit-cell's transfer matrix:

$$\mathbf{T} = e^{\frac{1}{2}i(\nu_+ - \nu_-)\Omega} \mathbf{Y}(\nu_+) \mathbf{Y}(-\nu_-) \quad (8)$$

For $\nu_+ = \nu_- = \nu$, the phase parameter $e^{\frac{1}{2}i(\nu_+ - \nu_-)\Omega}$ in the transfer matrix in Equation (8) cancels out as a consequence of equal and opposite Willis couplings, thus no skew angle emerges pertaining to a reciprocal dispersion relation. Following identical procedure to the development of Equation (6), the driven-wave dispersion relation of an elastic rod with alternating signs of Willis coupling is:

$$q = \pm \cos^{-1} \left(\nu^2 + (1 - \nu^2) \cos(\Omega) \right) \quad (9)$$

and, as expected, no phase shift in the wavenumber is observed. Non-zero values of ν open wavenumber bandgaps, centered around odd integer multiples of $q = \pm\pi$, and increasing ν 's magnitude yields larger gaps. To observe the wavenumber bandgaps, the solutions in Equation (9) are repeated periodically along the

wavenumber axis every 2π , necessarily yielding wavenumber bandgaps of *identical* width, with their lower and upper limits, respectively, being:

$$q_- = \pm \left[2(n-1)\pi + \cos^{-1}(2\nu^2 - 1) \right] \quad (10a)$$

$$q_+ = \pm \left[2n\pi - \cos^{-1}(2\nu^2 - 1) \right] \quad (10b)$$

which occur at the frequencies $\Omega = (2p-1)\pi$, where $p, n \in \mathbb{N}$ and \mathbb{N} is the set of natural numbers. Note that n denotes the order of the wavenumber bandgap and the pairs $q = \pm n\pi$ and $\Omega = (2p-1)\pi$ are points at which the linear dispersion lines of $\nu = 0$ case intersect. Using Equation (10), a formula for the identical wavenumber-bandgaps' width is deduced:

$$\Delta q = 2 \left(\pi - \cos^{-1} \left(2\nu^2 - 1 \right) \right) \quad (11)$$

Figure 3 shows band structure examples of a material with no Willis coupling (as the baseline) and with reversed-sign Willis couplings and $\nu = \pm 0.25, 0.5$, showing the emergence of wavenumber bandgaps as predicted by Equation (10). As can be seen, flipping the sign of ν does not affect the band structure as it results in a different choice of the unit cell. Further, complex frequencies values emerge in wavenumber bandgap [11], and the magnitude of the imaginary part grows larger with higher values of ν . The dispersion analyses are verified via the finite element method, which agrees excellently with the analytical predictions represented via the circles in the figure. For reference, the wavenumber bandgap limits q_{\pm} and corresponding width are also shown for swept range of ν . As ν approaches the limiting case of 1, the dispersion curves become vertical lines and the wavenumber-bandgap width peaks at $\Delta q = 2\pi$.

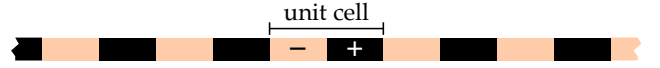


Figure 2: Schematic of an elastic rod with a unit cell of alternating negative/positive Willis coupling.

Similarities between reversed-sign Willis couplings and bi-layered periodicity

An interesting observation here is the resemblance between periodicity in Willis coupling and phononic crystals of two layers (1 and 2) with special modulation parameters in terms of the bandgap opening mechanism. It has been shown that frequency bandgaps in phononic crystals open with perfect periodicity and equal width by satisfying two conditions [12]:

- A zero frequency contrast, achieved via setting $\ell_{12}c_2 = \ell_{21}c_1$, and
- A non-zero characteristic impedance contrast $\beta = (z_1 - z_2)/(z_1 + z_2)$, where $z_{1,2} = A_{1,2}\sqrt{E_{1,2}\rho_{1,2}}$ are the characteristic impedance of the constitutive layers¹.

The functions governing the frequency-bandgap limits exhibit nearly identical resemblance with their wavenumber-bandgap counterpart, and, thus, the function for their width. Table 1 is compiled to concisely summarize these similarities for easier comparisons. As can be seen in the table, and apart from a 2

¹Note that all variables hold identical meaning to what has been defined in the article, and the subscript 1,2 are used to distinguish phononic crystal's two layers.

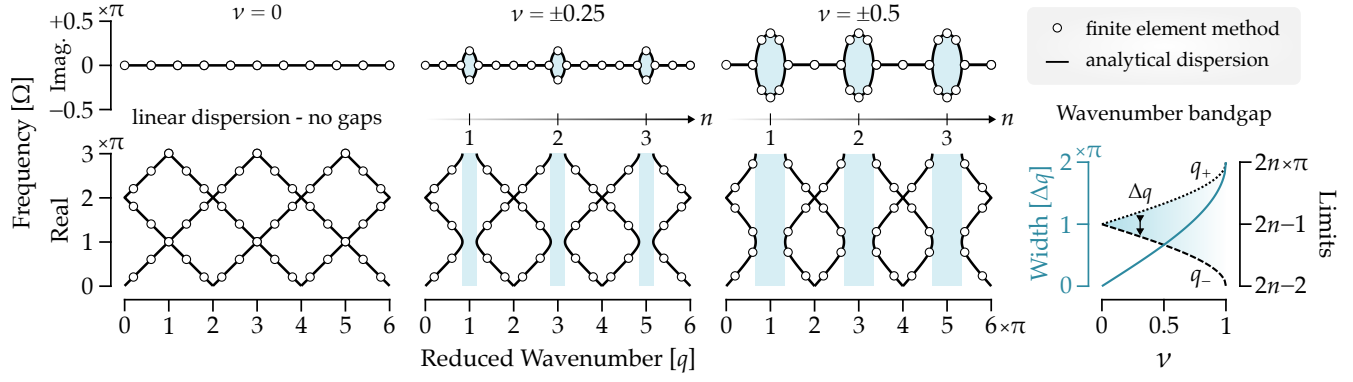


Figure 3: (left) Dispersion diagrams for the uniform rod with linear dispersion and no gaps case ($\nu = 0$) and a rod with Willis coupling of alternating signs and $\nu = \pm 0.25, \pm 0.5$. As can be seen, the wavenumber bandgaps open (shaded areas) whenever $\nu \neq 0$ and grows in size with increasing its magnitude, regardless of the sign. All orders of wavenumber bandgaps (denoted by n) have identical width. Frequencies are complex within said gaps and have larger imaginary values with higher $|\nu|$. Finite element simulation (depicted as circles) provides further validation to the analytical results. (right) Wavenumber-bandgap width Δq and limits q_{\pm} as a function of ν , corroborating the behavior of bandgap growth in the dispersion diagrams.

Table 1: Comparison between the expressions for the limits and width of wavenumber bandgaps for materials with periodic Willis couplings (Figure 2) and those of frequency bandgaps of a bi-layered phononic crystals with a zero frequency contrast and a non-zero impedance contrast [12].

Gap type	Lower limit	Upper limit	Width
Wavenumber	$q_- = 2(n-1)\pi + \cos^{-1}(2\nu^2 - 1)$	$q_+ = 2n\pi - \cos^{-1}(2\nu^2 - 1)$	$\Delta q = 2(\pi - \cos^{-1}(2\nu^2 - 1))$
Frequency	$\Omega_- = (n-1)\pi + \frac{1}{2}\cos^{-1}(2\beta^2 - 1)$	$\Omega_+ = n\pi - \frac{1}{2}\cos^{-1}(2\beta^2 - 1)$	$\Delta\Omega = \pi - \cos^{-1}(2\beta^2 - 1)$

multiplier for the wavenumber equations, the resemblance is so close and it is as if the parameters ν and q are swapped with β and Ω . As such, one may deduce that the role of impedance contrast in opening a *frequency* bandgap is equivalent to the role of the normalized modulation speed ν in opening a *wavenumber* bandgap, given reversed-sign Willis coupling.

Concluding remarks

The introduction of Willis coupling in elastic media traditionally yields non-reciprocal band structure due the presence of momentum bias. Peculiarly, reversing Willis-coupling signs is analytically proven to produce reciprocal band structures with wavenumber bandgaps, and analogies to bi-layered phononic crystals are noted. While physical motion of an elastic rod gives rise to Willis coupling, a feedback controller (e.g., Refs.[13–15]) could be an alternative route for realizing Willis coupling, especially if a periodic variation in Willis coupling is sought, which could open a future research direction.

¹M. A. Attarzadeh and M. Nouh, “Elastic wave propagation in moving phononic crystals and correlations with stationary spatiotemporally modulated systems”, *AIP Advances* **8**, 105302 (2018).

²J. A. Wickert and J. Mote C. D., “Classical Vibration Analysis of Axially Moving Continua”, *Journal of Applied Mechanics* **57**, 738–744 (1990).

³H. Nassar, X. Xu, A. Norris, and G. Huang, “Modulated phononic crystals: non-reciprocal wave propagation and willis materials”, *Journal of the Mechanics and Physics of Solids* **101**, 10–29 (2017).

⁴H. Nassar, A. N. Norris, and G. Huang, “Waves over a periodic progressive modulation: a python tutorial”, *arXiv preprint arXiv:2211.06294* (2022).

⁵H. B. Al Ba’ba’a, “Brillouin-zone definition in non-reciprocal Willis monatomic lattices”, *JASA Express Letters* **3**, 120001 (2023).

⁶M. I. Hussein, M. J. Leamy, and M. Ruzzene, “Dynamics of phononic materials and structures: Historical origins, recent progress, and future outlook”, *Applied Mechanics Reviews* **66**, 040802 (2014).

⁷Y.-F. Wang, Y.-Z. Wang, B. Wu, W. Chen, and Y.-S. Wang, “Tunable and active phononic crystals and metamaterials”, *Applied Mechanics Reviews* **72**, 040801 (2020).

⁸Y. Jin, Y. Pennec, B. Bonello, H. Honarvar, L. Dobrzynski, B. Djafari-Rouhani, and M. I. Hussein, “Physics of surface vibrational resonances: pillared phononic crystals, metamaterials, and metasurfaces”, *Reports on Progress in Physics* **84**, 086502 (2021).

⁹M. I. Hussein and M. J. Frazier, “Band structure of phononic crystals with general damping”, *Journal of Applied Physics* **108** (2010).

¹⁰G. Trainiti, Y. Xia, J. Marconi, G. Cazzulani, A. Erturk, and M. Ruzzene, “Time-Periodic Stiffness Modulation in Elastic Metamaterials for Selective Wave Filtering: Theory and Experiment”, *Physical Review Letters* **122**, 124301 (2019).

¹¹M. Moghaddaszhadeh, M. Attarzadeh, A. Aref, and M. Nouh, “Complex spatiotemporal modulations and non-hermitian degeneracies in \mathcal{PT} -symmetric phononic materials”, *Phys. Rev. Appl.* **18**, 044013 (2022).

¹²M. Nouh et al., “The role of frequency and impedance contrasts in bandgap closing and formation patterns of axially-vibrating phononic crystals”, *Journal of Applied Mechanics* **91** (2024).

¹³J. E. Pechac and M. J. Frazier, “Non-reciprocal supratransmission in mechanical lattices with non-local feedback control interactions”, *Crystals* **11**, 94 (2021).

¹⁴M. I. Rosa and M. Ruzzene, “Dynamics and topology of non-Hermitian elastic lattices with non-local feedback control interactions”, *New Journal of Physics*, 10.1088/1367-2630/ab81b6 (2020).

¹⁵H. Alli and T. Singh, “On the feedback control of the wave equation”, *Journal of Sound and Vibration* **234**, 625–640 (2000).